QUANTITATIVE ^{31}P NUCLEAR MAGNETIC RESONANCE ANALYSIS OF METABOLITE CONCENTRATIONS IN LANGENDORFF-PERFUSED RABBIT HEARTS

JANICE K. GARD,* GEORGE M. KICHURA,* JOSEPH J. H. ACKERMAN,* JOEL D. EISENBERG,‡ JOSEPH J. BILLADELLO,‡ BURTON E. SOBEL,‡ AND RICHARD W. GROSS‡

Department of Chemistry, College of Arts and Sciences, Washington University, St. Louis, Missouri 63130; and ‡Department of Medicine, School of Medicine, Washington University, St. Louis, Missouri 63110

ABSTRACT The quantitative analysis of the mobile high-energy phosphorus metabolites in isovolumic Langendorff-perfused rabbit hearts has been performed by ^{31}P NMR utilizing rapid pulse repetition to optimize sensitivity. Absolute quantification required reference to an external standard, determination of differential magnetization saturation and resonance peak area integration by Lorentzian lineshape analysis. Traditionally accepted hemodynamic indices (LVDP, dp/dt) and biochemical indices (lactate, pyruvate) of myocardial function were measured concomitantly with all NMR determinations. Hemodynamically and biochemically competent Langendorff-perfused rabbit hearts were found to have intracellular PCr, ATP, GPC, and P_i concentrations of 14.95 ± 0.25, 8.08 ± 0.13, 5.20 ± 0.58 and 2.61 ± 0.47 mM respectively. Intracellular pH was 7.03 ± 0.01. Cytosolic ADP concentration was derived from a creatine kinase equilibrium model and determined to be ~36 μM. Reduction of perfusate flow from 20 to 2.5 ml/min demonstrated statistically significant decreases in PCr, ATP, and pH as well as an increase in P_i that correlated closely with the independent hemodynamic and biochemical indices of myocardial function. The decrease in ATP and PCr concentrations precisely matched the increase in P_i during reduced flow. These results constitute the first quantitative determination of intracellular metabolite concentrations by ^{31}P NMR in intact rabbit myocardium under physiologic and low flow conditions.

INTRODUCTION

The detailed study of biochemical regulatory mechanisms and their time dependent response to physiological perturbations is greatly facilitated through quantification of intracellular metabolite concentrations utilizing a nondestructive dynamic technique such as NMR spectroscopy. Although ^{31}P NMR analysis of intact tissues has become a rapidly expanding field of biomedical research (1 and references therein) the ability of NMR to provide absolute, as opposed to relative, mobile metabolite concentrations has, in general, not been realized. Determination of absolute metabolite concentrations requires integration of full resonance lineshapes, analysis of magnetization saturation and, ultimately, comparison with an external standard.

NMR spectroscopy has been used in conjunction with several perfused heart models to examine myocardial response to a variety of physiologic perturbations. However, in the main, these studies have routinely expressed the observed metabolic alterations in terms of resonance peak heights or peak height ratios without consideration of full resonance lineshape integration or differential magnetization saturation. Furthermore, the heart perfusion protocols have often employed nonphysiologic perturbations such as the induction of anesthesia and anticoagulation prior to heart excision or have utilized nonphysiologic perfusion media (e.g., inclusion of EDTA or the absence of insulin and/or inorganic phosphate in the perfusate). The lack of strict hemodynamic control during the entire experimental period (e.g., cardiac pacing and ventricular preload) has additionally complicated interpretation of experimental results. Futhermore, most studies have employed zero flow (e.g., global ischemia) to simulate ischemia that differs markedly from the in vivo situation where residual flow is present in the ischemic zone through the collateral circulation. Finally, previous NMR investigations have not correlated independent hemodynamic and biochemical indices of myocardial function with quantitative alterations in intracellular ^{31}P metabolite concentrations and intracellular pH.

The present study utilizes ^{31}P NMR rapid pulse repetition methodology with subsequent magnetization saturation correction to quantify intracellular concentrations of

This paper was presented in preliminary form at the 187th National Meeting of the American Chemical Society, St. Louis, MO (April, 1984).

Correspondence should be addressed to Dr. Ackerman or Gross.

phosphorus metabolites in hemodynamically and biochemically competent isovolumic Langendorff-perfused rabbit hearts under control and low flow conditions. The perfusion model and experimental protocol employed avoid the difficulties mentioned above. This investigation demonstrates the excellent correlation of NMR derived metabolite concentrations with other independent indices of myocardial function measured concomitantly during the NMR experiment. These correlations validate the ^{31}P NMR experiment as a sensitive monitor of myocardial competence and provide quantitative data for future metabolic studies of intact myocardium.

MATERIAL AND METHODS

NMR Spectroscopy

A laboratory-built NMR probe based on modification of designs from the University of Oxford group of Radda, Gadian, and coworkers (2) was constructed to accommodate 4–7 g rabbit hearts in a vertical orientation (Fig. 1, see caption for details). The sample chamber had a 25 mm bore to avoid compression of the heart. A two turn Helmholtz style foil rf coil (30 mm diameter × 40 mm height), designed according to the optimized parameters of Hoult (3), was employed in the single-coil configuration (^{31}P 90° pulse width 85 μs at 100 W using 150 mM KCl with a point test sample of 85% H_3PO_4 in the coil center).

Experiments were performed at 80.98 MHz on a CXP 200 spectrometer (Bruker Instruments, Inc., Billerica, MA) in the absence of proton decoupling. To optimize signal-to-noise (4) an acquisition time slightly in excess of $3T_2^*$ for phosphocreatine (PCr), the resonance with the longest T_2^* relaxation time, was used with a 10° pulse without additional relaxation delays. Magnetic field homogeneity was optimized by shimming on the proton free induction decay through the ^{31}P rf coil (5). Spin-lattice relaxation times (T_1) were determined from peak intensity (height) measurements using the BASH saturation recovery technique (6, 7) with evolution period cycling. Experimentally determined magnetization saturation factors were obtained by comparison of spectra acquired under the above rapid repetition conditions with spectra acquired under slow repetition conditions where a 25 s relaxation delay was employed (>4 × longest measured metabolite T_1, that of glycerophosphorylcholine, GPC) with a 90° pulse width. All chemical shifts are reported relative to PCr as 0.0 ppm using the IUPAC recommended convention (8).

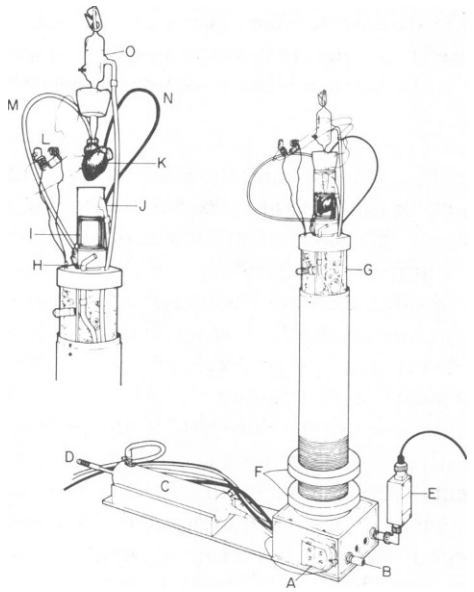

FIGURE 1 NMR probe for quantification of phosphorus metabolites in the perfused rabbit heart at 80.98 MHz. (*A*) thermocouple assembly; (*B*) rf input; (*C*) heat exchanger for input perfusate; (*D*) perfusate input; (*E*) rf trap on pacing input to isolate the DC stimulator from the NMR rf circuitry; (*F*) brass spacer rings for probe height adjustment; (*G*) copper-coated glass epoxy printed circuit board housing for electronics, grounding and tube segregation; (*H*) one of three air jets used to circulate warm air around the sample chamber; (*I*) 55 μm foil Helmholtz NMR coil; (*J*) sample chamber; (*K*) Langendorff-perfused heart; (*L*) additional rf tank traps for DC stimulator isolation; (*M*) pulmonary arterial cannula; (*N*) balloon-tipped catheter for pressure measurements; (*O*) perfusate input cannula-bubble trap.

Rabbit Heart Perfusion

2–3 kg male New Zealand white rabbits were stunned and killed by cervical dislocation. No additional anesthesia or blood anticoagulants were employed. The heart was rapidly excised and the aorta cannulated for retrograde perfusion with (EDTA free) Krebs-Henseleit perfusion medium (NaCl 118 mM, KCl 5.0 mM, $CaCl_2$ 2.5 mM, $MgSO_4$ 0.6 mM, KH_2PO_4 1.2 mM, dextrose 10 mM, $NaHCO_3$ 24 mM, Insulin 70 μu/ml). The perfusate was oxygenated with 95:5% oxygen/carbon dioxide and delivered at a flow rate of 20 ml/min. The inferior and superior venae cavae and pulmonary veins were ligated and the pulmonary artery was cannulated to allow collection and analysis of the coronary venous effluent. Two rf-isolated copper pacing leads were sutured to the right ventricle and the heart was paced at a rate of 180 beats/min throughout all experiments. A balloon-tipped catheter was placed into the left ventricle via the left atrial appendage which provided a constant preload of 8–12 mm Hg and allowed continuous monitoring of heart rate, left ventricular developed pressure (LVDP) and the first derivative of the pressure (dp/dt). The heart was placed in the NMR probe and additional perfusion medium was added to fill the sample tube to improve spectral resolution. The entire procedure took 15–20 min.

Criteria for inclusion in the study were based on spectral, metabolic, and hemodynamic parameters. Hearts with initial spectra showing peak height ratios of PCr/ATP > 2, ATP/total inorganic phosphate >1.5, lactate concentration in the effluent <2 mg % and left ventricular pulse pressure >60 mm Hg were included in the study. The NMR indices were never the sole determinant for inclusion. ~10–15% of all hearts perfused were rejected according to the above criteria.

Data Analyses

A capillary tube containing 1 M hexachlorocyclotriphosphazene (trimer) in C_6D_6 with 62 mM chromium acetylacetonate was mounted on the inner side of the sample chamber and used as an intensity reference standard as previously described (9). This intensity standard was calibrated by comparison against known concentrations of NaH_2PO_4 solutions in 150 mM KCl in various-sized spherical glass chambers centered in the NMR sample holder and surrounded by 150 mM KCl solution. In all cases, the electrical damping characteristics of the calibrating samples were similar to those of the perfused heart preparation.

An acquisition time (70 ms) ≥ $3T_2^*$ for PCr ensured that all resonance lineshapes were not distorted, as other metabolite T_2^* values were substantially shorter. All free induction decays were zero filled to 2,048 total data points prior to Fourier transformation.

The Lorentzian lineshape resulting from a first order single exponential decay results in substantial signal intensity in the wings of the peak, far from the center of the resonance. Levy and coworkers have stressed the need for substantial integration limits in accurately determining NMR resonance peak areas (10). Weiss and Ferretti (11) have further shown that, in cases of limited signal-to-noise, a Lorentzian lineshape analysis (curve fit and analytical—closed form—area determination) can provide increased accuracy over digital integration techniques. In cases where

resonance lines overlap (i.e., PCr and γ-phosphate of ATP) a lineshape analysis can be used to obtain individual peak areas. For purposes of quantitative analysis herein, various regions of the ^{31}P spectrum were fit to a sum of Lorentzian lines plus a single straight line by a nonlinear least squares fitting routine using a finite difference Levenberg Marquardt algorithm run on a VAX 11/780 computer (Digital Equipment Corp., Maynard, MA). Inclusion of a straight line in the lineshape analysis was found to provide an excellent first order correction to baseline nonidealities.

The resonance from the β-phosphate of ATP (taken to be unique for ATP) was fit to a single Lorentzian line while the peaks due to PCr and the γ-phosphate of ATP were fit to two Lorentzian lines. The spectral region containing resonances from phosphomonoesters (PME), inorganic phosphate (P_i), and GPC was fit to from three to five Lorentzian lines, depending on the apparent number of peaks present. Concentrations measured directly herein for this spectral region are those of total P_i (intra- and extracellular), and GPC. Since the lineshape and resolution of the PME spectral region was poorly defined (especially during reduced flow) no quantitative results are reported for it. Because of signal-to-noise and resolution limitations, both P_i and GPC quantification was performed on spectra representing the sum of three time blocks, namely 4–16 min (control period), 20–32 (reduced flow), and 36–48 min (reflow).

The chemical shift of P_i with respect to PCr (δ_o) as a function of pH was determined utilizing a physiologic solution (KCl 150 mM, KH_2PO_4 20 mM, PCr 10 mM, ATP 5 mM, $MgCl_2$ 9.25 mM) at 37°C. These data were combined with previously obtained values (Ackerman, J. J. H., unpublished results; 12) and fitted to the Henderson-Hasselbach/chemical-shift expression, Eq. 1 (13), resulting in pK = 6.79, δ_A = 3.25 and δ_B = 5.75.

$$pH = pK - \log_{10}[(\delta_o - \delta_B)/(\delta_A - \delta_o)] \quad (1)$$

Here, pK describes the equilibrium, $H_2PO_4^- \rightleftarrows HPO_4^= + H^+$, and δ_A, δ_B are the ^{31}P chemical shifts of the acid and base phosphate forms. As has been discussed previously, the pH determined by ^{31}P NMR is accurate to ±0.1 and pH changes are accurate to at least ±0.05 (14).

Pulmonary arterial effluent was collected during the NMR experiments and samples were analyzed for lactate and pyruvate concentrations by standard analytical procedures (15).

Experimental Protocol

NMR data were accumulated in a series of consecutive 4-min time blocks (3,480 free induction decays) extending over 48 min. Left ventricular pressure was monitored continuously and midway through each time block the dp/dt was determined. After termination of each experiment the hearts were blotted dry, weighed, and heated to constant weight at 110°C for determination of tissue water. Sample temperature regulation was calibrated at 36–37°C for each flow rate.

Control hearts (normal flow, 20 ml/min) were followed without additional perturbation over the full time course. Midway through each odd time block a sample of pulmonary arterial effluent was obtained.

In the reduced flow studies the perfusate flow was decreased at the end of the fourth time block (16 min) to either 5 ml/min (25% flow—data not shown) or 2.5 ml/min (12.5% flow), and then increased to normal flow (reflow) at the end of the eighth time block (32 min). Hearts were observed over four additional time blocks after reflow. During the control and reflow periods of the reduced flow studies the pulmonary arterial effluent was collected during odd-numbered time blocks; effluent was collected during each 25% flow time block and (due to insufficient flow) over both the combined first and second, and third and fourth, 12.5% flow time blocks. Effluent samples were stored at −70°C prior to lactate and pyruvate analysis.

In the proceeding discussion the following notation has been adopted. The term "control study" refers to the group of 14 hearts that were examined over 48 min with no change in normal perfusate flow rate from 20 ml/min. The term "control period" refers to the 16 min period (four 4-min time blocks) at the start of all studies (control, 25% flow, and 12.5% flow) in which the perfusate flow was maintained at 20 ml/min. All error limits are given as standard error of the mean (SEM) unless specifically indicated to be standard deviation (SD). Statistical significance was accepted at 95% confidence limits, $P \leq 0.05$.

RESULTS AND DISCUSSION

^{31}P NMR Spectra of Isolated Perfused Rabbit Hearts

A ^{31}P NMR spectrum of a perfused rabbit heart obtained utilizing the probe and acquisition conditions described in materials and methods is shown in Fig. 2. Additional acquisition parameters and identification of resonances are provided in the figure caption. The apparent frequency resolution limit is given by the linewidth of the PCr resonance that averaged 27 Hz for all hearts examined. (In a later study, a greater emphasis on B_0 homogeneity optimization reduced the average PCr linewidth to 19 Hz.) Signal-to-noise compares favorably with other previously published ^{31}P NMR spectra of perfused rabbit heart.

Magnetization Saturation

The directly measured and derived (via T_1, vide infra) magnetization saturation factors are given in Table I and agree within 9% (excluding GPC). The measured values were consistently greater than the derived values. Measurement of T_1 was independent of the saturation factor measurement as each determination employed a separate

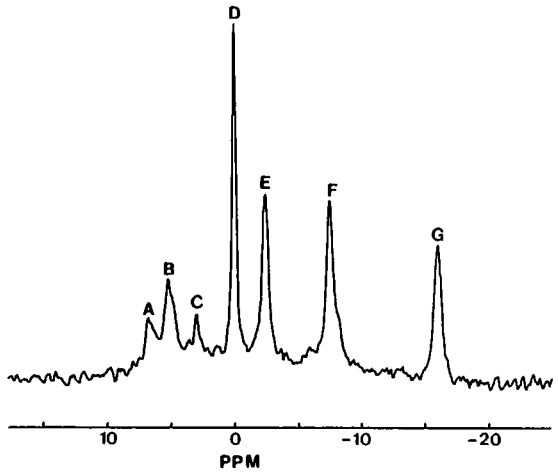

FIGURE 2 P-31 control period NMR spectrum of a Landendorff-perfused, isovolumic rabbit heart (~6 g, 37°C) at 80.98 MHz. Spectrum represents 4 min of data averaging (3,480 scans, 10° pulses, 7,463 Hz spectral width, 1,024 total data points zero filled to 2,048 points, 15 Hz exponential line broadening filter applied). No proton decoupling was employed. Intracellular phosphocreatine (PCr) is taken as 0.0 ppm and IUPAC convention is used to define chemical shifts (8). Peak assignments are: (*A*) phosphomonoesters (PME); (*B*) inorganic phosphate (P_i); (*C*) glycerophosphorylcholine (GPC); (*D*) PCr, (0.0 ppm); (*E*) γ-phosphate of ATP and β-phosphate of ADP; (*F*) α-phosphate of ATP and ADP; shoulder to lower chemical shift is due to NAD; (*G*) β-phosphate of ATP. The external reference (trimer) peak is not shown; it occurs just off scale at 25.3 ppm (see ref. 9).

TABLE I
MEASURED AND DERIVED SPIN-LATTICE RELAXATION TIMES (T_1) AND MAGNETIZATION SATURATION FACTORS*

Metabolite resonance	Measured saturation factor‡ (s ± SEM)	Derived saturation factor§	Measured T_1‖ (s ± SEM)	Derived T_1¶ (s)	Solution T_1** (s ± SD)
β-phosphate of ATP	7.7 ± 0.6 (n = 11)	7.4	1.23 ± 0.05 (n = 7)	1.5	2.57 ± 0.08 (n^* = 3)
α-phosphate of ATP	8.3 ± 0.2 (n = 11)	7.3	1.19 ± 0.07 (n = 7)	2.0	2.8 ± 0.3 (n^* = 3)
γ-phosphate of ATP	8.8 ± 0.4 (n = 11)	7.9	1.63 ± 0.09 (n = 11)	2.4	3.20 ± 0.08 (n^* = 3)
phosphocreatine	10.7 ± 0.2 (n = 11)	9.2	2.7 ± 0.2 (n = 11)	4.0	8.0 ± 0.4 (n^* = 3)
glycerophosphorylcholine	17.0 ± 0.6 (n = 9)	12.8	5.7 ± 0.5‡‡ (n = 10)	9.2	8.5 ± 1.2 (n^* = 3)
total inorganic phosphate§§	11.1 ± 0.5 (n = 10)	10.4	3.7 ± 0.1 (n = 11)	4.3	11.6 ± 0.9 (n^* = 3)
phosphomonoesters	14.5 ± 2.1 (n = 10)	—	—	7.1	—

*Hearts used for T_1 measurements were not used for saturation factor measurements. Only a single T_1 or saturation factor measurement was made on a given heart and these hearts were not used for other experiments. Measurements were made under control perfusate flow conditions, 20 ml/min.
‡The measured ratio of the resonance area under slow repetition conditions (90° pulse, $T \geq 4\ T_1$) to the resonance area under fast repetition conditions (9.7° pulse, T = 70 ms).
§The ratio of M_o to M_{xy} as determined by Eq. 2 substituting T = 70 ms, α = 9.7° and T_1 = the measured values given in this table.
‖Measured by the BASH saturation recovery method (6, 7) with evolution period cycling.
¶Derived from Eq. 2 assuming the ratio of M_o to M_{xy} under rapid repetition conditions (T = 70 ms, α = 9.7°) is equal to the measured saturation factor. This is the equivalent of a two-point T_1 measurement.
**T_1 measurements at 37°C on a pH = 7.31 physiologic solution of the following composition: PCr 10.6 mM, KCl 150.0 mM, KH_2PO_4 10.3 mM, GPC 2.0 mM, ATP 5.0 mM, $MgSO_4$ 5.1 mM. Value reported is the average of three T_1 determations (n^* = 3) on the same solution.
‡‡Measured T_1 distribution was bimodal: 7.1 ± 0.2 (n = 5), 4.2 ± 0.3 (n = 5).
§§Attempts to determine values for both intra- and extracellular inorganic phosphate were unsuccessful because of insufficient linewidth resolution.

group of rabbits. Thus the concordance between measured and derived saturation factors supports the accuracy of these determinations.

Under the conditions employed herein, the exponential form of the saturation factor (4) can be accurately approximated as a linear function of T_1,

$$\frac{M_o}{M_{xy}} = \left(\frac{1 - \cos\alpha}{T \cdot \sin\alpha}\right)(T_1) + \frac{\cos\alpha}{\sin\alpha}, \qquad (2)$$

where advantage was taken of the fact that since the pulse repetition period $T \ll T_1$ one can approximate $\exp(-T/T_1)$ as $1 - (T/T_1)$. For a flip angle of 10° and T = 70 ms Eq. 2 becomes

$$\frac{M_o}{M_{xy}} = 1.3\ T_1 + 5.7\ . \qquad (3)$$

Therefore (as can be seen in Table I), because of the small slope to intercept ratio a 49% change in the T_1 of the γ-phosphate of ATP (1.63 to 2.43 s) would result in only an 11% difference in saturation factor (7.9 to 8.8); similarly, a 48% change in the T_1 of PCr (2.7 to 4.0 s) would result in only a 16% (9.2 to 10.7) difference in saturation factor.

This moderate dependence of saturation factor on T_1 under the rapid repetition conditions employed herein has two important ramifications. First, small errors in measured saturation factor lead to large errors in T_1 derived from such measurements as in Table I. Second, one would have to postulate major changes in T_1 and/or in the rates of chemical exchange modulation of effective T_1 to markedly change the degree of magnetization saturation during the course of an experiment. No evidence of such change was seen during the course of study described herein. Nevertheless, it remains an important assumption of this rapid pulse repetition methodology that saturation factors determined under control conditions remain constant or undergo minor change relative to metabolite concentration changes under noncontrol conditions.

The metabolite T_1 values of a physiologic solution, shown for comparison in Table I, are all substantially greater (100–200%) than those of the perfused rabbit heart. This may be due to the presence of cytosolic paramagnetic ions, exchange between bound (immobile) and free (mobile) metabolites, or perhaps substantial differences in viscosity.

Lineshape Analysis

Four separate spectral regions of all ^{31}P spectra were independently fit, each to a sum of Lorentzian lines plus a single straight line. Fitted regions were chosen such that the resonance intensities were just above the noise level at

the region's frequency limits. The result of a multiparameter Lorentzian lineshape analysis of the ^{31}P spectrum shown in Fig. 3 *a* is given in Fig. 3 *b*, where the calculated lineshapes have been substituted into the original spectrum within the fitted regions only. Potential primary sources of error include both deviations from true Lorentzian lineshape and incorrect phasing of the spectrum (i.e., dispersive in addition to absorptive components). Quantitative comparison between fitted and experimental data is shown in Fig. 3 *c* (i.e., the difference spectrum of Fig. 3 *a* minus Fig. 3 *b*). Deviations from an ideal fit are small, typically of the same intensity as the noise level in the original data. In fact, had the entire theoretical spectrum been subtracted (as opposed to the specifically fitted regions), the errors in the lineshape analysis would not have been discernable from the background noise. Comparison of other randomly chosen spectra gave similar results. Thus, the use of a Lorentzian lineshape analysis is justified. Further justification may be found in the close agreement in ATP concentration whether determined independently from the β-phosphate or the γ-phosphate resonance area (i.e., a difference between the two determinations of 0.1 ± 0.1 μmol/g-wet-weight (n = 160), vide infra).

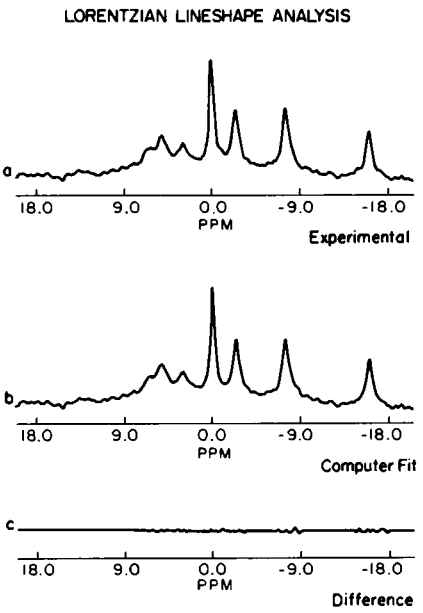

FIGURE 3 Results of a Lorentzian lineshape analysis of a control period heart spectrum. The original experimental spectrum is shown in *a*. Specific spectral regions were then defined along with the number of peaks in each region and estimates of the peaks' position, height, and width; a nonlinear least-squares lineshape analysis was then performed for each region and the resulting lineshape (i.e. simulated spectrum) substituted back into the original spectrum within the previously defined spectral regions (*b*). A difference spectrum, $a - b = c$, shown in *c* illustrates the quality of the fit. Errors in the curve fitting are within the original baseline noise.

Phosphorus Metabolites

The control period concentrations of ATP, PCr, P_i, and GPC were 3.23, 5.98, 1.04, and 2.08 μmol/g-wet-weight (Table II). Resolution of the intra- and extracellular P_i resonances was not sufficient for separate quantitative area determination of each component. For comparison, Table III lists the values of total ATP, PCr, and ADP determined independently by other researchers using freeze-extraction techniques with in vitro perfused rabbit heart (16–21).

ATP and PCr concentrations determined by NMR fall in the upper range of freeze extraction derived concentrations. This possibly results from the documented deleterious effects of the finite freezing time on high energy phosphorus metabolite levels using Wollenberger clamps (22). Our inability to directly measure ADP concentrations by ^{31}P NMR, 0.1 ± 0.1 μmol/g-wet-weight (n = 160) (taken as the difference between the concentrations determined from the resonances at −2.5 ppm (nucleoside di- and triphosphates) and −16 ppm [nucleoside triphosphates]) suggests that the substantial amounts of ADP detected by freeze-extraction (~0.5 μmol/g-wet-weight; Table III) represent either a bound, immobilized pool or an artifact of finite freezing times (1).

TABLE II
CONTROL PERIOD MOBILE METABOLITE CONCENTRATIONS AS DETERMINED BY ^{31}P NMR

	Metabolite					
	ATP	PCr	P_i	GPC	ADP*	pH‡
	(n = 160)	(n = 160)	(n = 35)	(n = 35)	(—)	(n = 77)
μmol/g-wet-weight:	3.23	5.98	1.04§	2.08	0.017‖ 0.012‖	7.03
±SEM	±0.05	±0.10	±0.19	±0.23	—	0.01
cytosolic¶ mM:	8.08	14.95	2.61	5.20	0.042 0.030	—
±SEM	±0.13	±0.25	±0.47	±0.58	—	—

*Derived two different ways from consideration of the creatine kinase equilibrium reaction; see text.
‡Intracellular pH.
§Value represents cytosolic P_i only; see text.
‖Values represents cytosolic ADP only; see text.
¶Derived values of actual intracellular cytosolic concentrations; see text.

TABLE III

TOTAL IN VITRO PERFUSED* RABBIT HEART TISSUE METABOLITE CONCENTRATIONS AS DETERMINED BY FREEZE-CLAMPING AND CHEMICAL ANALYSIS

μmol/g-wet-weight ± SEM			Reference
ATP	ADP	PCr	
2.75 ± 0.27 (n = 5)	0.46 ± 0.05 (n = 5)	5.54 ± 0.17 (n = 6)	Lee and Visscher (16)‡
2.67 ± 0.14 (n = 8)	—	6.62 ± 0.30 (n = 8)	Thomas et al. (17)‡
3.55 ± 0.24 (n = 6)	0.57 ± 0.09 (n = 6)	—	Richman and Wyborny (18)§
2.66 ± 0.22 (n = 4)	—	—	Aussedat and Rossi (19)‡
2.62 ± 0.26 (n = 6)	0.48 ± 0.05 (n = 6)	—	Liu and Feinberg (20)‡
2.89 ± 0.19 (n = 6)	—	5.15 ± 0.25 (n = 6)	Nayler et al. (21)‡

*Perfusion media were not reported to contain insulin.

‡Data originally presented as μmol/g-dry-weight and converted to μmol/g-wet-weight by dividing by the wet to dry weight ratio determined in the current investigation for control study hearts: 6.37 ± 0.19 (n = 14).

§Data originally presented as μmol/g-wet-weight.

Reduced Flow Conditions

Reduction of perfusate flow resulted in significant PCr, Pi, and H^+ concentration changes compared with the control study (Fig. 4). The PCr concentration decreased 69% from 6.5 ± 0.4 to a plateau level of 2.0 ± 0.4 μmol/g-wet-weight after 16 min of reduced flow. The H^+ concentration rapidly increased 2.6-fold from pH 7.01 ± 0.03 to 6.60 ± 0.03. Total inorganic phosphate concentration increased from 4.0 ± 0.3 to 9.5 ± 0.8 μmol/g-wet-weight. This corresponds to a 6.5-fold increase in cytosolic inorganic phosphate (vide infra) from 1.0 ± 0.3 to 6.5 ± 0.8 μmol/g-wet-weight. After 16 min of reflow the PCr, Pi, and H^+ levels returned to control period values: PCr 6.8 ± 0.4 μmol/g-wet-weight, pH 7.00 ± 0.03, total P_i 4.2 ± 0.3 μmol/g-wet-weight. A similar pattern of change to a new steady-state level during reduced flow with subsequent return toward control period levels after reflow was mirrored in the left ventricular developed pressure, peak dp/dt, and pulmonary arterial effluent lactate and pyruvate concentrations (Fig. 5). However the recovery of hemodynamic parameters appeared to lag behind the rapid recovery of the metabolic indices (i.e., PCr, P_i, H^+, lactate, pyruvate). None of the metabolic or hemodynamic parameters, including PCr concentration, exhibited any marked overshoot of control period values after reflow. Phosphocreatine concentration overshoot immediately after recovery from zero flow has been reported previously (23–30).

The effect of reduced flow upon ATP levels was much less than for the other metabolites, as expected from consideration of the creatine kinase reaction. After 16 min of reduced flow ATP concentrations dropped from 3.3 ± 0.1 to 2.4 ± 0.2 μmol/g-wet-weight a decrease of 27%. This decrease was significantly different from the control study. Subsequent reflow gradually returned values toward control levels but after 16 min ATP had not returned to control concentrations.

The decrease in the sum of ATP and PCr levels was precisely matched by the increase in P_i during reduced flow, −5.4 and +5.5 μmol/g-wet-weight respectively. This is consistant with PCr and ATP hydrolysis as the primary source of P_i.

The GPC resonance was located in a region of great peak overlap. However, a previous comparison from this laboratory of freeze-clamp wet-chemical analysis of GPC concentration with NMR analysis, using control period hearts not employed in this study, showed no significant difference between the GPC levels determined by either method (31). In this study glycerophosphorylcholine levels appeared to decrease during reduced flow from 1.8 ± 0.1 to 1.3 ± 0.2 μmol/g-wet-weight ($0.1 < p < 0.2$).

As can be seen from Figs. 4 and 5, metabolite levels, pH, and hemodynamic parameters were quite stable over 48 min in the control study and in the 16 min control periods prior to the reduced flow studies. Compared with the control study the values of all observables in the control periods of the reduced flow studies were not significantly different.

Derived Cytosolic Concentrations

The directly measured metabolite concentrations are determined by ^{31}P NMR as total (mobile) moles per wet weight of tissue, however, these values can be converted to intracellular cytosolic concentrations. Nayler et al. (32) and others (33–35) have shown that ~60% of the tissue volume of a buffer perfused rabbit heart is intracellular space, and furthermore, that ~20% can be attributed to mitochondrial space. Thus, assuming a density of 1 gram/ml, 40% of the tissue wet-weight in grams represents the

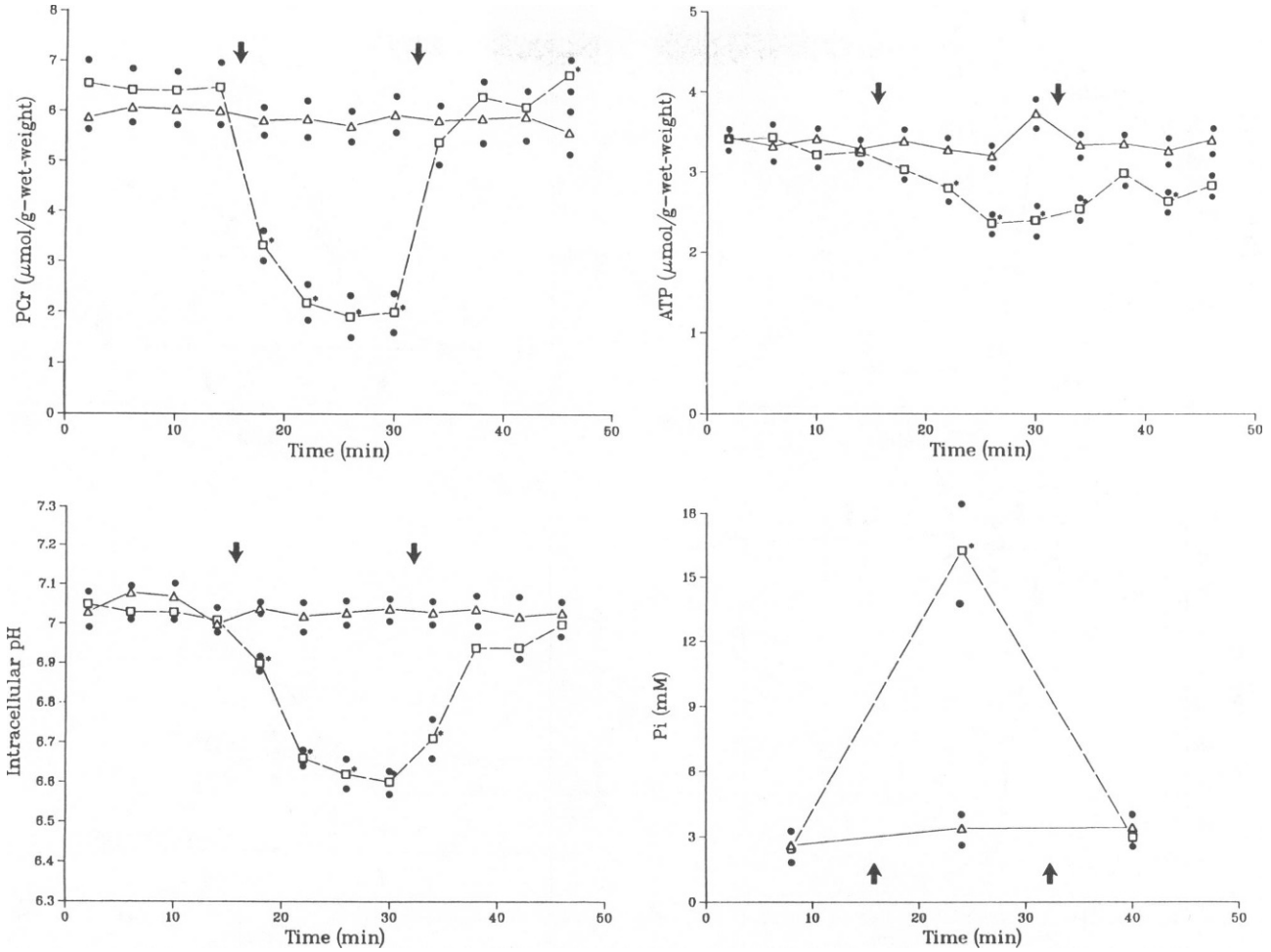

FIGURE 4 Mean metabolite concentrations determined by ^{31}P NMR under control, reduced flow and reflow periods. Phosphocreatine (PCr) and adenosine triphosphate (ATP) are reported, as measured, in micromoles per gram-wet-weight. Inorganic phosphate (P_i) is reported as millimolar cytosolic P_i to stress its derivation from measured total P_i; this can be converted to cytosolic P_i per gram-wet-weight by multiplying by 0.4 (see text for details). Intracellular H^+ concentration is reported in pH units and was determined from the P_i chemical shift. The arrows indicate the reduction of flow at 16 min and the return to control flow at 32 min for the 12.5% (2.5 ml/min) flow study, □, $n = 14$. There was no reduction of flow during the control study (20 ml/min), △, $n = 14$. Standard error of the mean is indicated by ● and significant deviation ($P < 0.05$) from the control study is denoted by *.

nonmitochondrial intracellular cytosolic volume in milliliters. Given that the observed ATP, PCr, and GPC are primarily cytosolic intracellular metabolites, this conversion is straightforward. Control period cytosolic concentrations of ATP, PCr, and GPC are 8.08, 14.95, and 5.20 mM respectively (Table II).

The P_i concentration obtained from ^{31}P NMR contains contributions from not only intracellular, interstitial, and vascular spaces, but also a contribution from the perfusion medium surrounding the heart. Since, to a good approximation, small ions are equally distributed between interstitial and vascular space (36), one may reasonably approximate interstitial and vascular P_i concentrations as 1.2 mM, equal to that of the perfusion medium. With this assumption, and given the previously discussed compartment volume distribution and the sensitive volume of the NMR probe (19.6 ml), the intracellular cytosolic P_i concentration can be derived. The control period value is 2.61 mM (Table II).

Attempts to measure ADP concentration directly by ^{31}P NMR failed (vide supra). However, a free cytosolic ADP concentration can be derived from consideration of the creatine kinase reaction. Work of several groups supports an equilibrium model for the creatine kinase reaction in heart (37–40) and other tissue (41, 42). Utilizing the known equilibrium constant for the creatine kinase reaction, 5.5×10^{-10} (43), and the known total creatine pool concentration, 24.5 mM (17)[1], the derived cytosolic ADP concentration is 30 μM.

[1]Data originally presented as μmole/g-dry-weight. Converted to millimoles per liter by dividing by the wet-to-dry-weight ratio (see footnote *b* in Table III) and dividing by 0.4 to account for the 40% cytosolic volume. See text for details.

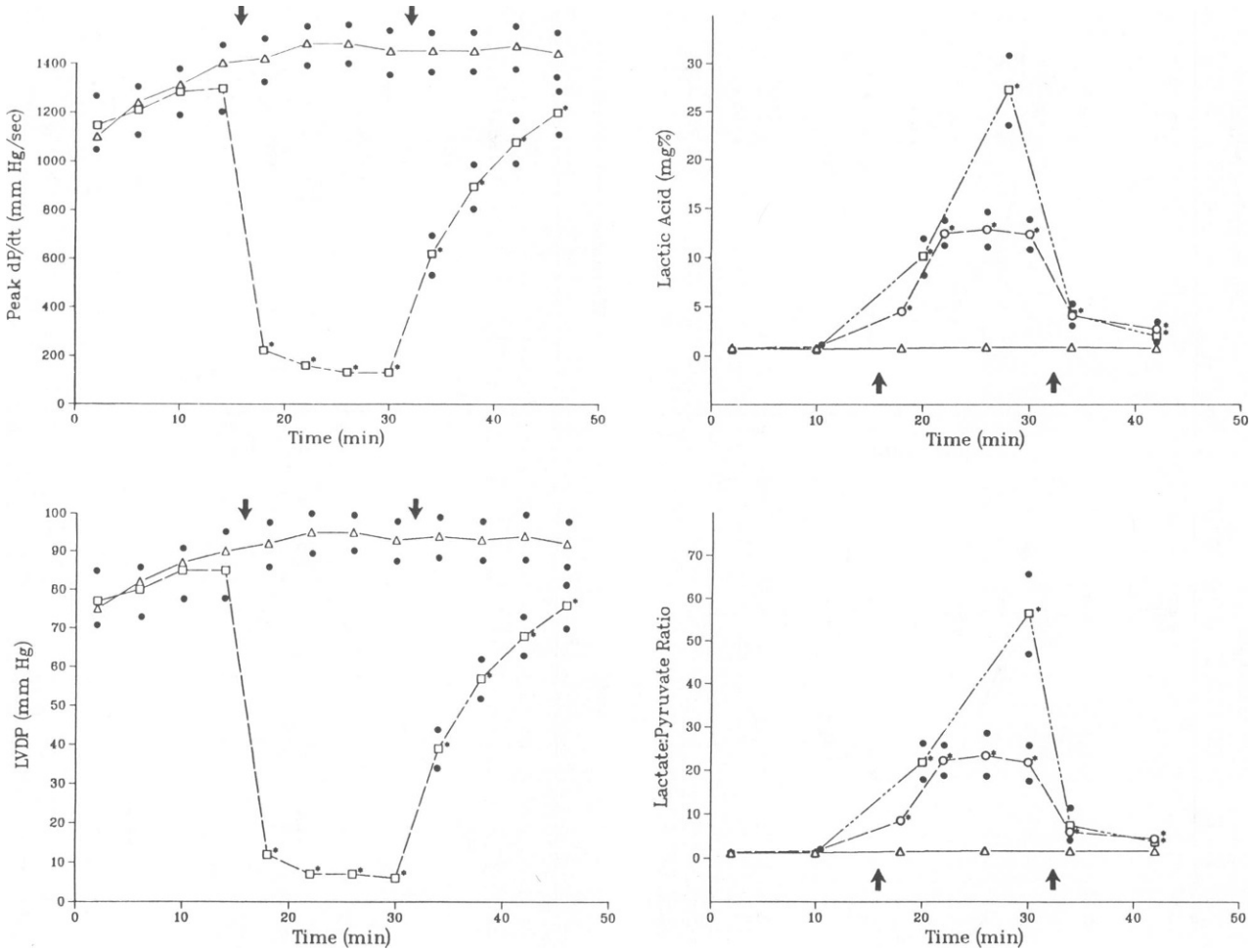

FIGURE 5 Mean hemodynamic and left ventricular effluent metabolite levels as a function of time during control (20 ml/min, $n = 14$, Δ) and 12.5% flow studies (2.5 ml/min, $n = 14$, □). Left ventricular (LVDP) developed pressure and peak dp/dt reported in millimeters of mercury (mm Hg) and mm Hg/s, respectively. The lactic acid and lactic acid-to-pyruvic acid ratio of the pulmonary arterial effluent are also shown for the 25% flow study (5 ml/min, $n = 12$, ○). Arrows indicate the reduction of flow at 16 min and return to control flow at 32 min for the reduced flow studies. Standard error of the mean is denoted by ● and significant deviations ($P < 0.05$) from the control study by *. In cases where error limits are not shown the error was within the given symbol.

Alternatively, the mass action expression can be rearranged to yield a linear formulation, Eq. 4, given an equilibrium model with the following assumptions: (*a*) the equilibrium constant has the previously cited value (43); (*b*) the cytosolic free (unbound) ADP concentration is constant; and (*c*) the total free cytosolic pool of creatine plus phosphocreatine (TCP) is constant.

$$\frac{[H^+]}{(5.5 \times 10^{-10})[ATP]} = \frac{[TCP]}{[ADP][PCr]} - \frac{1}{[ADP]}. \quad (4)$$

A plot of $[H^+]/(5.5 \times 10^{-10})[ATP]$ as a function of $[PCr]^{-1}$ is then predicted to yield an intercept of $-[ADP]^{-1}$ and a slope of $[TCP]/[ADP]$. Thus, this model not only predicts a linear formulation, Eq. 4, but provides a measure of the free cytosolic ADP concentration, i.e., $-(\text{intercept})^{-1}$, and a measure of the total pool of creatine plus phosphocreatine, i.e., − slope/intercept. Using the mean cytosolic concentrations derived from the 25% flow study for H^+, ATP, and PCr, Eq. 4 yields a linear correlation factor (r) of 0.88 ($n = 12$, $P < 0.001$), [ADP] = 0.042 mM, and [TCP] = 26.2 mM. This ADP concentration compares favorably with the 0.030 mM derived above as does the total creatine pool with the previously cited value directly measured in rabbit heart by Lee and Visscher (16).

These results support the validity of the proposed "linear" creatine kinase equilibrium model under control and 25% flow conditions. It should be noted that the (two) data points that lie most clearly off the linear regression line represent time blocks 5 and 9, namely, the initial 4 min of reduced flow and the initial 4 min of reflow. These time blocks represent periods of dramatic, rapid metabolic and hemodynamic flux (Figs. 4 and 5). Thus, it is not surprising that the proposed equilibrium model is least satisfactory during intervals of change between steady-state conditions. However, this model did not agree well with the

12.5% flow study data suggesting that the creatine kinase reaction may not rapidly return to equilibrium and/or that the free ADP concentration does not remain constant after dramatic reductions in substrate delivery.

A parameter of substantial importance in cellular energy regulation is the free energy of ATP hydrolysis at pH = 7 ($\Delta G'$), Eq. 5,

$$\Delta G' = \Delta G^{o\prime} + RT\ln \frac{[ADP][P_i]}{[ATP]}. \quad (5)$$

Using the cytosolic concentrations of ATP, ADP, and P_i given in Table II and a $\Delta G^{o\prime}$ value of -31.8 KJ/mol from Lawson and Veech (44) one derives $\Delta G' = -60.7$ KJ/mol. This is similar but somewhat higher than $\Delta G'$ values of -53.6 KJ/mol and -58.8 KJ/mol previously reported for perfused rat heart (45, 46) primarily due to the small ADP concentration.

The low concentrations of mobile ADP (0.030 and 0.042 mM) are certainly well below ^{31}P NMR detection limits in perfused heart and are consistent with our inability to directly measure ADP levels (vide supra). These concentrations are very close to the experimentally determined values of the Michaelis constant ($K_{M_{ADP}}$) of ADP for respiratory stimulation (47–49). Strong evidence has been presented (47–49) that respiratory rates can be influenced by the concentration of extramitochondrial ADP and the kinetics of its transport. It has been previously pointed out that the similarity between the derived values for the free concentration of ADP and the reported values of the $K_{M_{ADP}}$ suggests an important regulatory role for this molecule in myocardial respiration (29).

Independent Hemodynamic and Biochemical Indices

Motivated by the potential future clinical application of ^{31}P NMR for diagnosis and management of cardiovascular disease, strong correlates between NMR derived metabolite concentrations (i.e., ATP, PCr, P_i, and H^+) and accepted traditional indices of heart function (i.e., LVDP, LVP, dp/dt, lactate, and lactate/pyruvate ratio) are noted. Considering both reduced flow experiments, PCr and P_i concentrations correlated extremely well with all hemodynamic parameters ($|r| \geq 0.96$). Furthermore, the P_i concentration correlated very closely with lactate level and the lactate:pyruvate ratio ($|r| \geq 0.97$) while PCr concentration showed a more moderate relationship ($|r| \geq 0.92$). The proton concentration showed a greater correlation with the hemodynamic parameters, lactate concentration, and lactate/pyruvate ratio in the 25% flow experiment ($|r| \geq 0.87$) than in the 12.5% flow experiment ($|r| \geq 0.69$). The slow rate of ATP decline in the presence of rapid hemodynamic deterioration resulted in a poor correlation of ATP concentration with the hemodynamic and pulmonary arterial effluent parameters in both the 25% flow experiment ($|r| \geq 0.45$) and the 12.5% flow experiment ($|r| \geq 0.62$). Therefore, given the entire time period of the reduced flow model presented herein, one can rank the NMR-derived metabolite concentrations as indices of cardiac function in order of strong to weak linear correlates as PCr $\simeq$ P_i > $H^+ \gg$ ATP.

Summary

Quantitative phosphorus metabolite analysis has been performed on isovolumic Langendorff-perfused rabbit hearts by ^{31}P NMR. The salient features of this model were as follows. (*a*) Blood anticoagulant and chemical anesthesia were not employed; animals were stunned prior to heart excision. (*b*) The perfusion medium was EDTA free but did contain insulin and inorganic phosphate. (*c*) 16-min periods of reduced perfusate flow (20 ml/min reduced to 5 or 2.5 ml/min) were used in contrast to periods of zero flow (i.e., "global ischemia"). (*d*) Hearts were continuously paced at 180 beats/min throughout all experiments including reduced-flow periods. (*e*) Hemodynamic, and pulmonary arterial effluent lactate and pyruvate measurements were made concomitantly with NMR data collection on all hearts. (*f*) A complete protocol of control experiments was carried out and analyzed in full over the entire experimental time course. (*g*) Resonance peak areas were determined by Lorentzian lineshape analysis and converted to concentration units by consideration of magnetization saturation and reference to an external standard.

The NMR derived ATP and PCr concentrations agree well with those derived by chemical extraction. However, at variance with extract results, NMR derived ADP levels are extremely low. Excellent linear correlations are observed between the phosphorus metabolite levels and independent hemodynamic and biochemical indices of myocardial function. The quantitative ^{31}P NMR experiment is, thus, a sensitive monitor of myocardial competence and, therefore, ^{31}P NMR can potentially provide information to facilitate the clinical evaluation and management of cardiovascular disease.

This work was supported by Washington University Intramural funds, the Washington University Computer Center, National Institutes of Health (NIH) grant GM 30331, and National Science Foundation grant CHE 8100211.

We acknowledge use of NMR software provided by George Levy of Syracuse University, NIH Biotechnology Research Resource grant RR 01317. This work represents a portion of the Ph.D. thesis of J. K. Gard, submitted to the University of Illinois, Urbana-Champaign (1984).

Received for publication 4 October 1984 and in final form 15 April 1985.

REFERENCES

1. Balaban, R. S. 1984. The Application of nuclear magnetic resonance to the study of cellular physiology. *Am. J. Physiol.* 246:C10–C19.
2. Gadian, D. G. 1982. Nuclear magnetic resonance and its application to living systems. Clarendon Press, Oxford. 11.
3. Hoult, D. I. 1978. The NMR receiver: a description and analysis of design. *Progr. Nucl. Magn. Reson. Spectrosc.* 12:41–77.

4. Becker, E. D., J. A. Ferretti, and P. N. Gambhir. 1979. Selection of optimum parameters for pulse fourier transform nuclear magnetic resonance. *Anal. Chem.* 51:1413–1420.
5. Ackerman, J. J. H., D. G. Gadian, G. K. Radda, and G. G. Wong. 1981. Observation of ^{1}H NMR signals with receiver coils tuned for other nuclides. *J. Magn. Reson.* 42:498–500.
6. Markley, J. L., W. J. Horsley, and M. P. Klein. 1971. Spin-lattice measurements in slowly relaxing complex spectra. *J. Chem. Phys.* 55:3604–3605.
7. Becker, E. D., J. A. Ferretti, R. K. Gupta, and G. H. Weiss. 1980. The choice of optimal parameters for measurement of spin-lattice relaxation times. II. Comparison of saturation recovery, inversion recovery, and fast inversion recovery experiments. *J. Magn. Reson.* 37:381–394.
8. IUPAC recommendations on NMR spectra. 1976. *Pure Appl. Chem.* 45:219.
9. Gard, J. K., and J. J. H. Ackerman. 1983. A ^{31}P NMR external reference for intact biological systems. *J. Magn. Reson.* 51:124–127.
10. Sotak, C. H., C. L. Dumoulin, and G. C. Levy. 1983. Software for quantitative analysis by carbon-13 Fourier transform nuclear magnetic resonance spectrometry. *Anal. Chem.* 55:782–787.
11. Weiss, G. H., and J. A. Ferretti. 1983. Accuracy and precision in the estimation of peak areas and NOE factors. *J. Magn. Reson.* 55:397–407.
12. Gadian, D. G. Cited in Jacobus, W. E., I. M. Pores, S. K. Lucas, C. H. Kallman, M. L. Weisfeldt, and J. T. Flaherty. 1982. The role of intracellular pH in the control of normal and ischemic myocardial contractility: A ^{31}P nuclear magnetic resonance and mass spectrometry study. R. Nuccitelli and D. W. Deamer, editors. Intracellular pH: its measurement, regulation, and utilization in cellular functions. Alan R. Liss, Inc., New York. 548.
13. Jacobus, W. E., I. M. Pores, S. K. Lucas, C. H. Kallman, M. L. Weisfeldt, and J. T. Flaherty. 1982. The role of intracellular pH in the control of normal and ischemic myocardial contractility: A ^{31}P nuclear magnetic resonance and mass spectrometry study. R. Nuccitelli and D. W. Deamer, editors. Intracellular pH: its measurement, regulation, and utilization in cellular functions. Alan R. Liss, Inc., New York. 537–565.
14. Gadian, D. G. 1983. Whole organ metabolism studied by NMR. *Annu. Rev. Biophys. Bioeng.* 12:69–89.
15. Sigma Technical Bulletin No. 726-UV, June 1981. Pyruvic Acid and Lactic Acid.
16. Lee, Y. C. P., and M. B. Visscher. 1970. Perfusate cations and contracture and Ca, Cr, PCr, and ATP in rabbit myocardium. *Am. J. Physiol.* 219:1637–1641.
17. Thomas, G. E., S. Levitsky, and H. Feinberg. 1983. Chlorpromazine inhibits loss of contractile function, compliance, and ATP in ischemic rabbit heart. *J. Mol. Cell. Cardiol.* 15:621–628.
18. Richman, H. G., and L. Wyborny. 1964. Adenine nucleotide degradation in rabbit heart. *Am. J. Physiol.* 207:1139–1145.
19. Aussedat, J., and A. Rossi. 1975. Nucleotides adenyliqires libres due coeur de lapin isole et perfuse. *C.R. Seances Soc. Biol. Ses Fil.* 170:124–129.
20. Liu, M. S., and H. Feinberg. 1971. Incorporation of adenosine-8-^{14}C and inosine-8-^{14}C into rabbit heart adenine nucleotides. *Am. J. Physiol.* 220:1242–1248.
21. Nayler, W. G., R. Ferrari, and A. Williams. 1980. Protective effect of pretreatment with verapamil, nifedipine, and propranolol on mitochondrial function in the ischemic and reperfused myocardium. *Am. J. Cardiol.* 46:242–248.
22. Gilbert, C., K. M. Kretzschmar, D. R. Wilkie, and R. C. Walesize. 1971. Chemical change and energy output during muscular contraction. *J. Physiol. (Lond.)* 218:163–193.
23. Bailey, I. A., and A. M. Seymour. 1981. The effects of reperfusion on the ^{31}P NMR spectrum of ischemic rat hearts. *Biochem. Soc. Trans.* 9:234–236.
24. Bailey, I. A., A. M. C. Seymour, and G. K. Radda. 1981. A ^{31}P-NMR study of the effects of reflow on the ischaemic rat heart. *Biochim. Biophys. Acta.* 637:1–7.
25. Seymour, A. M. C., I. A. Bailey, and G. K. Radda. 1983. A protective effect of insulin on reperfusing the ischaemic rat heart shown using ^{31}P-NMR. *Biochim. Biophys. Acta.* 762:525–530.
26. Jaffin, J. H., G. J. Magovern, Jr., K. R. Kanter, J. T. Flaherty, T. J. Gardner, and W. E. Jacobus. 1981. Improved myocardial metabolism with oxygenated perfluorocarbon cardioplegia. *Surg. Forum.* 32:290–293.
27. Flaherty, J. T., J. H. Jaffin, G. J. Magovern, Jr., K. R. Kanter, T. J. Gardner, and M. V. Miceli. 1984. Maintenance of aerobic metabolism during global ischemia with perfluorocarbon cardioplegia improves myocardial preservation. *Circulation.* 69:585–592.
28. Flaherty, J. T., M. L. Weisfeldt, B. H. Bulkley, T. J. Gardner, V. L. Gott, and W. E. Jacobus. 1982. Mechanisms of ischemic myocardial cell damage assessed by phosphorus-31 nuclear magnetic resonance. *Circulation.* 65:561–571.
29. Flaherty, J. T., M. L. Weisfeldt, D. P. Hollis, H. V. Schaff, V. L. Gott, and W. E. Jacobus. 1980. Mass spectrometry and phosphorus-31 nuclear magnetic resonance demonstrate additive myocardial protection by potassium cardioplegia and hypothermia during global ischemia. *Adv. Myocardiol.* 2:487–499.
30. Brooks, W. M., and R. J. Willis. 1983. ^{31}P nuclear magnetic resonance study of the recovery characteristics of high energy phosphate compounds and intracellular pH after global ischemia in the perfused guinea pig heart. *J. Mol. Cell. Cardiol.* 15:495–502.
31. Billadello, J. J., J. K. Gard, J. J. H. Ackerman, and R. W. Gross. 1984. Determination of intact tissue glycerophosphorylcholine levels by quantitative ^{31}P-nuclear magnetic resonance spectroscopy and correlation with spectrophotometric quantification. *Anal. Biochem.* 144:269–274.
32. Nayler, W. G., A. Slade, E. M. V. Williams, and C. E. Yepez. 1980. Effect of prolonged β-adrenoceptor blockade on heart weight and ultrastructure in young rabbits. *Br. J. Pharmacol.* 68:363–371.
33. Johnson, J. A., and M. A. Simonds, 1962. Chemical and histological space determinations in rabbit heart. *Am. J. Physiol.* 202:589–592.
34. Strome, D. R., R. L. Clamay, and N. C. Gonzalez. 1977. Determinants of transmembrane bicarbonate flux during acid-base changes. *J. Appl. Physiol.* 43:925–930.
35. Saari, J. T., and J. A. Johnson. 1971. Decay of calcium content and contractile force in the rabbit heart. *Am. J. Physiol.* 221:1572–1575.
36. Berne, R. M., and M. N. Levy. 1972. Cardiovascular Physiology. C.V. Mosby Company, St. Louis, MO, 111.
37. Matthews, P. M., J. L. Bland, D. G. Gadian, and G. K. Radda. 1982. A ^{31}P-NMR saturation transfer study of the regulation of creatine kinase in the rat heart. *Biochim. Biophys. Acta.* 721:312–320.
38. Jacobus, W. E., and A. L. Lehninger. 1973. Creatine kinase of rat heart mitochondria. *J. Biol. Chem.* 248:4803–4810.
39. Matthews, P. M., J. L. Bland, D. G. Gadian, and G. K. Radda. 1981. The steady-state rate of ATP synthesis in the perfused rat heart measured by ^{31}P NMR saturation transfer. *Biochem. Biophys. Res. Commun.* 103:1052–1059.
40. Saks, V. A., G. B. Chernousova, D. E. Gukovsky, V. N. Smirnov, and E. I. Chazov. 1975. Studies of energy transport in heart cells. *Eur. J. Biochem.* 57:273–290.
41. Balaban, R. S., H. L. Kantor, and J. A. Ferretti. 1983. In Vivo flux between phosphocreatine and adenosine triphosphate determined by two-dimensional phosphorus NMR. *J. Biol. Chem.* 258:12787–12789.
42. Veech, R. L., J. W. R. Lawson, N. W. Cornell, and H. A. Krebs. 1979. Cytosolic phosphorylation potential. *J. Biol. Chem.* 254:6538–6547.
43. DeFuria, R. A., J. S. Ingwall, E. T. Fossel, M. K. Dygert, W. E.

Jacobus, and J. S. Ingwall, editors. 1981. Heart Creatine Kinase: The Integration of Isozymes for Energy Distribution. Williams and Wilkins, Baltimore. 135–141.

44. Lawson, J. W. R., and R. L. Veech. 1979. Effects of pH and free Mg^{+2} on the K_{eq} of the creatine kinase reaction and other phosphate hydrolyses and phosphate transfer reactions. *J. Biol. Chem.* 254:6528–6537.

45. Matthews, P. M., S. R. Williams, A. M. Seymour, A. Schwartz, G. Dube, D. G. Gadian, and G. K. Radda. 1982. A ^{31}P-NMR study of some metabolic and functional effects of the inotropic agents epinephrine and ouabain, and the ionophore R02-2985 (X537A) in the isolated, perfused rat heart. *Biochim. Biophys. Acta.* 720:163–171.

46. Kauppinen, R. A., J. K. Hiltunen, and I. E. Hassinen. 1980. Subcellular distribution of phosphagens in isolated perfused rat heart. *FEBS (Fed. Eur. Biochem. Soc.) Lett.* 112:273–276.

47. Chance, B., and G. R. Williams. 1955. Respiratory enzymes in oxidative phosphorylation. *J. Biol. Chem.* 217:283–293.

48. Jacobus, W. E., R. W. Moreadith, and K. M. Vandegaer. 1982. Mitochondrial respiratory control. *J. Biol. Chem.* 257:2397–2402.

49. Jacobus, W. E., R. W. Moreadith, and K. M. Vandegaer. 1983. Control of heart oxidative phosphorylation by creatine kinase in mitochondrial membranes. *Ann. NY Acad. Sci.* 414:73–89.